Modeling cell volume regulation in nonexcitable cells: the roles of the Na^+ pump and of cotransport systems

JULIO A. HERNÁNDEZ AND ERNESTO CRISTINA
Sección Biofísica, Facultad de Ciencias, Universidad de la República, 11400 Montevideo, Uruguay

Hernández, Julio A., and Ernesto Cristina. Modeling cell volume regulation in nonexcitable cells: the roles of the Na^+ pump and of cotransport systems. *Am. J. Physiol.* 275 (*Cell Physiol.* 44): C1067–C1080, 1998.—The purpose of this study is to contribute to understanding the role of Na^+-K^+-ATPase and of ionic cotransporters in the regulation of cell volume, by employing a model that describes the rates of change of the intracellular concentrations of Na^+, K^+, and Cl^-, of the cell volume, and of the membrane potential. In most previous models of dynamic cellular phenomena, Na^+-K^+-ATPase is incorporated via phenomenological formulations; the enzyme is incorporated here via an explicit kinetic scheme. Another feature of the present model is the capability to perform short-term cell volume regulation mediated by cotransporters of KCl and NaCl. The model is employed to perform numerical simulations for a "typical" nonpolarized animal cell. Basically, the results are consistent with the view that the Na^+ pump mainly plays a long-term role in the maintenance of the electrochemical gradients of Na^+ and K^+ and that short-term cell volume regulation is achieved via passive transport, exemplified in this case by the cotransport of KCl and NaCl.

mathematical models; cell dynamics; electrochemical gradients

MANY DYNAMIC PROPERTIES OF cells are determined by the integrated functioning of cell membrane transport processes. As a classic example, the generation of the electrical potential difference across the plasma membrane of animal cells (V_m) is the result of the interaction of several passive and active processes of ionic transport (8, 29, 49). Under steady-state conditions, the resting V_m can be approximated by rather straightforward physicochemical formulations of the diffusive and electrogenic components (7, 17, 22, 24, 28, 41, 42, 53). However, a description of the temporal behavior is more complex and usually consists of systems of several nonlinear differential equations governing the rates of change of the membrane potential, of the cell volume, and of some intracellular ionic concentrations (29, 33, 34, 50, 55). These systems are generally difficult to analyze, and their study is mainly restricted to numerical simulations of transient and/or periodic changes in the membrane potential of excitable and nonexcitable cells. The complexity of these models is a consequence of the fact that, in living cells, the transport of ions across the cell membrane simultaneously affects the cell volume (via effects on the intracellular osmolarity) and the V_m (via the generation of diffusive and/or electrogenic potentials) (29, 56). As one possible simplification, several authors have assumed that the cell volume remains constant during the course of electrical membrane phenomena (33, 34, 50). Still, this simplification does not permit the mathematical difficulties to be completely overcome, especially those emerging from the basic, nonlinear character of the ionic flux equations, in which the voltage dependence is determined by both linear and exponential terms (17, 24, 29, 49).

The Na^+-K^+-ATPase of the plasma membrane plays key roles in most dynamic responses of cells. In excitable cells, the onset of action potentials and the subsequent electrical recovery of the cell membrane occur by abrupt changes in the electrical currents of Na^+ and K^+, in turn determined by steep conductance changes and by the preexistence of electrochemical gradients for these ions. For the case of nerve cells, it has been classically recognized that the Na^+ pump mainly plays a long-term role in the maintenance of the electrochemical gradients of Na^+ and K^+; the enzyme can indeed be inhibited with no substantial effect on the development of action potentials for a considerable period (e.g., see Ref. 8). On the contrary, in cardiac cells, significant modification of the intra- and extracellular concentrations of Na^+ and K^+ may take place in the course of action potentials (34). Hence, the Na^+ pump plays a crucial role in the membrane repolarization that follows, to promptly restore ionic concentrations to the normal physiological levels that afterward guarantee the generation of a new action potential (33, 34). In both excitable and nonexcitable cells, the Na^+ pump plays diverse other roles associated with membrane and other cellular phenomena (6, 16, 47, 48), among them the maintenance of cell volume (5, 8).

The mechanisms involved in the regulation of cell volume fall into two main categories, long-term and short-term cell volume regulation (5, 20). Under normal isotonic conditions, all cells exhibit mechanisms to counter the natural tendency to increase intracellular tonicity. This tendency results from passive processes that can be basically interpreted in terms of a Gibbs-Donnan equilibrium (5, 8). In animal cells, characterized by distensible membranes, the passive tendency to gain diffusible cations, and hence to increase the cell volume by osmotically coupled water entry, is mainly counterbalanced by the Na^+ pump (5, 8). Under the standard mode of operation characterized by a 3 Na^+:2 K^+:1 ATP stoichiometric ratio, the enzyme extrudes one diffusible cation per cycle, thus contributing to reducing the amount of osmotically active intracellular solutes. The experimental evidence suggests that, under isotonic conditions, this protective device provided by the Na^+ pump mainly represents a "long-term" mechanism of regulating the cell volume (37). A rather explicit model capable of describing the long-term dynamic events that follow the "shutting off" of the Na^+ pump was advanced by Jakobsson (29).

Short-term cell volume regulation induced by anisosmotic shocks represents another characteristic ex-

0363-6143/98 $5.00

ample of dynamic phenomena in cells. The acute regulatory responses of cells to ambient perturbations of the osmotic pressure are widely distributed throughout the entire biological world (20, 31a, 62). Despite the large spectrum of ionic and nonionic solutes involved, these responses exhibit common dynamic features (5, 20). Basically, the cells respond to the cellular volume increase produced by acute hyposmotic shocks by augmenting the efflux of a highly concentrated intracellular species. Osmotic equilibrium is thus achieved by intracellular water loss and concomitant cell volume recovery [regulatory volume decrease (RVD)]. Conversely, a hyperosmotic medium results in a compensatory entry of a diffusive species, followed by osmotically driven water influx [regulatory volume increase (RVI)]. Although the elucidation of the basic role of short-term cell volume regulation under physiological conditions and of the primary mechanisms determining it remain matters of active investigation and discussion (3, 11, 20, 21, 45), it is nevertheless clear that this cellular response constitutes a ubiquitous and highly conserved way of reacting against a changing environment (9, 26, 31). The literature on the mathematical modeling of short-term cell volume regulation is not abundant (see, for instance, Ref. 58) and mainly consists of the incorporation of the phenomenon into the description of the overall properties of transport exhibited by specific cellular types (35, 55, 60, 61). A mathematical analysis of the dynamic aspects of the short-term regulatory response per se was performed by Weinstein (58) for the case of an epithelial cell transporting two electroneutral solutes and water. The author employed thermodynamic formalism to study the steady-state and time-dependent behavior of the system and to perform numerical calculations for a model of a urinary epithelium.

The purpose of this study is to contribute to understanding the role of Na^+-K^+-ATPase and of cotransport systems in the dynamic behavior of nonexcitable symmetrical cells, particularly cell volume regulation. Although this enzyme has been involved, directly or indirectly, in diverse cellular processes (see above), we focus here on its direct effects on the ionic concentrations, the cell volume, and the membrane potential. For this, we introduce a mathematical model describing the rates of change of the intracellular concentrations of Na^+, K^+, and Cl^- ($[Na^+]_i$, $[K^+]_i$, and $[Cl^-]_i$), of the cell volume (V_c), and of the V_m. Taken together, these five physicochemical variables might constitute the minimum set of variables necessary for an appropriate description of the basic dynamic properties of symmetrical animal cells (29). In contrast to most previous models of dynamic cellular phenomena (29, 35, 50, 55, 58, 60, 61), in which Na^+-K^+-ATPase is incorporated via phenomenological formulations, in the present work the enzyme is incorporated via an explicit kinetic scheme (10). This kinetic model has been employed, for instance, as a plausible alternative to describe the electrogenic contribution of the Na^+ pump (22) and to analyze repolarization in cardiac cells (34). Another feature of the cell model studied here is the capability of performing the characteristic responses of short-term cell volume regulation, RVD and RVI. In this model, these responses are mediated by a cell swelling-induced electroneutral flux of KCl (for RVD) and by a cell shrinkage-induced electroneutral flux of NaCl (for RVI). In view of its complexity (see above), the model is employed to illustrate, by means of numerical simulations, the behavior of a "typical" nonpolarized animal cell. Some particular issues considered here are *1*) the dependence of the reference state (steady state) on the activity of the Na^+ pump, *2*) the role of the enzyme and of the cotransporters of KCl and NaCl in long-term and short-term cell volume regulation, and *3*) the enzyme contribution to cell recovery after anisosmotic shocks. In general, the results are consistent with the view that the enzyme mainly plays a long-term role in the maintenance of the electrochemical gradients of Na^+ and K^+, whereas short-term cell volume regulation is mainly handled by the passive transport systems. Also, some results suggest that the electrogenic properties of the enzyme may underlie signaling events in cells.

Glossary

Variables

V_c	Cell volume
m_{Na}, m_K, m_{Cl}	Intracellular masses of Na^+, K^+, and Cl^-
V_m	Electrical potential difference across cell membrane
t	Time

Parameters

A_c	Effective permeant area of cell surface
P_{Na}, P_K, P_{Cl}	Permeability coefficients of Na^+, K^+, and Cl^-
P_w	Osmotic permeability
v^-, v^+	"Threshold" values of cell volume
Q^*_{Na}, Q^*_K	Kinetic parameters of cell volume-induced fluxes
$[Na^+]_e$, $[K^+]_e$, $[Cl^-]_e$, $[X]_e$	Extracellular concentrations of Na^+, K^+, Cl^-, and impermeant solute under isotonic conditions
τ	Time delay of cell volume regulatory responses
Π_e	Total extracellular solute concentration under isotonic conditions
r	Osmolarity ratio
X_i	Total amount of intracellular impermeant solute
N	Total Na^+-K^+-ATPase membrane density
$[ATP]_i$, $[ADP]_i$, $[P_i]_i$	Intracellular concentrations of ATP, ADP, and P_i

$k_{12}, \cdots, k_{61}$	Rate constants of transitions 12, $\cdots$, 61
$k_{16}, \cdots, k_{21}$	Rate constants of transitions 16, $\cdots$, 21
K_{eq}	Equilibrium (dissociation) constant of the reaction ATP $\leftrightarrow$ ADP + P_i

MATHEMATICAL MODEL

The cell model employed here to derive the mathematical model has the following general characteristics (Fig. 1; see also introduction).

Assumption 1. The cell is nonpolarized. In fact, several nonpolar cell types have been demonstrated to exhibit short-term cell volume regulation (see, for instance, Refs. 11, 19, 31).

Assumption 2. The changes in the V_c are determined by the net water movement between the extracellular and intracellular compartments, as a response to the generation of osmotic gradients across the cell membrane. The total solute concentration of the extracellular compartment remains constant. The cell contains a fixed intracellular amount of an anionic impermeant species (X_i), which, for simplicity, we assume to be monovalent. As an approximation, we assume that the total intracellular osmolarity is given by the sum of the concentrations of Na^+, K^+, Cl^-, and the impermeant species. We also assume ideal osmotic behavior for all the species. In contrast to previous models in which the assumption of instant osmotic equilibrium is employed to determine cell volume changes (29, 35, 55, 58), the present work considers the water flow explicitly.

Assumption 3. The plasma membrane contains diffusive paths for Na^+, K^+, and Cl^- (ionic channels) and a Na^+ pump with a fixed 3 Na^+:2 K^+ stoichiometric ratio. In APPENDIX A, we derive expressions for the steady-state fluxes of Na^+ and K^+ mediated by the enzyme, from the analysis of an explicit kinetic model (10, 22, 34) (Fig. 2). The employment of these expressions in the overall dynamic model implicitly assumes that the enzyme reaction achieves the steady-state condition on a different time scale than the V_c or the ionic intracellular concentrations. This has been a usual procedure in previous models of macroscopic dynamic phenomena incorporating explicit kinetic schemes of transport systems (33, 34, 59).

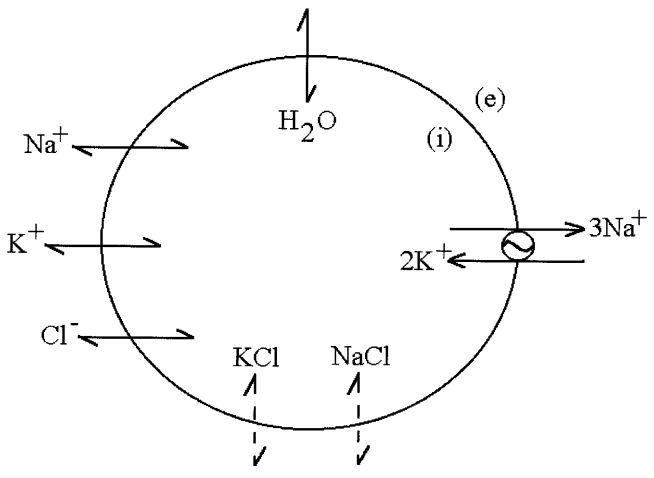

Fig. 1. Cell scheme representing diverse fluxes taking place across plasma membrane (i, intracellular; e, extracellular). Scheme includes Na^+-K^+-ATPase with 3 Na^+:2 K^+ stoichiometric ratio, diffusive paths for Na^+, K^+, Cl^-, and water (solid arrows), and cell volume-induced NaCl and KCl fluxes (dashed arrows).

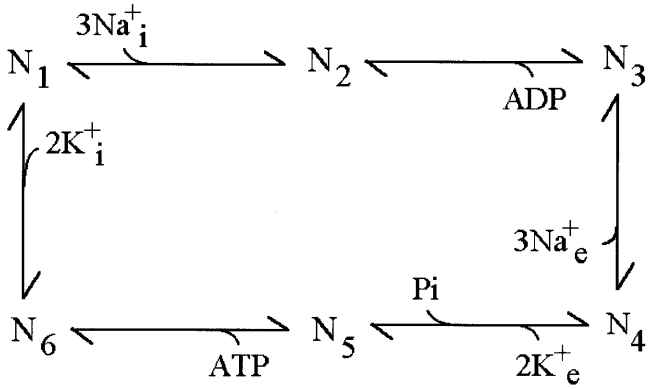

Fig. 2. State diagram of process of transport of Na^+ and K^+ mediated by Na^+-K^+-ATPase (after Ref. 10). $N_1, \cdots, N_6$ are intermediate states of enzyme. Na_i^+, K_i^+, Na_e^+ and K_e^+ are intracellular and extracellular Na^+ and K^+, respectively.

Assumption 4. Cell volume regulation is mediated by coupled fluxes of K^+ and Cl^- (for RVD) and of Na^+ and Cl^- (for RVI). In many animal cells, RVD is mediated by the loss of K^+ and Cl^-, whereas RVI is achieved by an interaction of transport systems leading to a net gain of Na^+, K^+, and Cl^- (for references, see Refs. 5, 20). Although, in most cases, the individual ionic fluxes appear to be uncoupled (2, 12, 25), we assume here that they are coupled via electroneutral cotransport systems. Under a hyposmotic shock, V_c increases. We assume that, when V_c reaches a threshold value v^+ ($v^+ >$ reference V_c), a sudden activation of systems leading to a net efflux of KCl takes place. Conversely, we assume that a shrinkage-induced influx of NaCl is triggered when V_c reaches the threshold value v^- ($v^- <$ reference V_c). In previously published models incorporating short-term cell volume regulation, the acute responses are mediated by volume-induced stepwise modifications of the basal ionic permeabilities (55, 58). We explore here a formulation in which the regulatory paths are independent of the basal ionic channels and remain inactive under reference conditions. These transport systems are turned on by cell volume changes and, as mentioned, determine electroneutral fluxes of KCl (for RVD) and NaCl (for RVI), in the form of cotransport systems. Once activated, these systems are modulated by the cell volume (see below). Indeed, there is evidence that some of these cotransport systems are implicated in the regulatory responses of diverse cell types (for references, see Ref. 5). The molecular mechanisms underlying these abrupt changes in the ionic fluxes and their dependence on the cell volume are not considered here. A plausible mechanism for determining modifica-

tions of the permeabilities mediating the regulatory responses is that the change in the concentration of the intracellular macromolecules constitutes the primary signal (38).

Assumption 5. The total area of the cell surface available for solute and water transport (A_c) remains constant and independent of the changes in cell volume. This approximation can be justified by assuming that all solute and water transport processes are mediated by integral membrane proteins, present in amounts that do not change in the course of cell volume modifications.

Under *assumptions 1–5*, the following mathematical model governs the rates of change of V_c, of m_{Na}, m_K, and m_{Cl}, and of V_m (defined as intracellular potential − extracellular potential)

$$\begin{aligned} dm_{Na}/dt &= A_c(-3J_p + J_{Na} + \phi_{Na}) \\ dm_K/dt &= A_c(2J_p + J_K + \phi_K) \\ dm_{Cl}/dt &= A_c(J_{Cl} + \phi_{Na} + \phi_K) \end{aligned} \qquad (1a)$$

$$dV_c/dt = (A_c V_w P_w)[(X_i + m_{Na} + m_K + m_{Cl})/V_c - \Pi_e]$$

To obtain the time dependence of V_m, we employed a stationary solution of the electroneutral condition (APPENDIX B)

$$J_p + J_{Na} + J_K - J_{Cl} = 0 \qquad (1b)$$

In *Eqs. 1a* and *1b*, the cycle flux J_p is defined by *Eq. A1*; J_{Na}, J_K, and J_{Cl} are the corresponding electrodiffusive fluxes, and ϕ_{Na} and ϕ_K are the cell volume-induced fluxes of NaCl and KCl, respectively. V_w is the partial molar volume of water, and the rest of the symbols represent parameters and variables listed in the *Glossary*. From inspection of *Eqs. 1a* and *1b*, one promptly notices that, under nonregulatory conditions of the cell volume (that is, for $\phi_{Na} = \phi_K = 0$), the steady state requires equivalence of the magnitudes of the active and passive fluxes of Na^+ and K^+, electrochemical equilibrium of Cl^-, and the condition of osmotic equilibrium. As is the usual practice in physicochemical models of integrated membrane transport processes, the model does not include terms describing the development of transmembrane tension.

The basal electrodiffusive fluxes of Na^+, K^+, and Cl^- are given by the Goldman expression (17), as modified by Hodgkin and Katz (24)

$$\begin{aligned} J_{Na} &= P_{Na}\epsilon_m\{[Na^+]_e \exp(-u/2) - (m_{Na}/V_c)\exp(u/2)\} \\ J_K &= P_K\epsilon_m\{[K^+]_e \exp(-u/2) - (m_K/V_c)\exp(u/2)\} \\ J_{Cl} &= P_{Cl}\epsilon_m\{[Cl^-]_e \exp(u/2) - (m_{Cl}/V_c)\exp(-u/2)\} \end{aligned} \qquad (2)$$

with $u = FV_m/RT$ and $\epsilon_m = u/[\exp(u/2) - \exp(-u/2)]$ and where F is Faraday's constant, R is the gas constant, and T is the absolute temperature in kelvin.

We assume that the cell volume-induced fluxes mediating the short-term regulatory responses are given by

$$\begin{aligned} \phi_{Na} &= Q_{Na}\{[Na^+]_e[Cl^-]_e - (m_{Na}m_{Cl}/V_c^2)\} \\ \phi_K &= Q_K\{[K^+]_e[Cl^-]_e - (m_K m_{Cl}/V_c^2)\} \end{aligned} \qquad (3)$$

For the physiological range of V_c values, we assume that Q_{Na} and Q_K depend on V_c according to

$$\begin{aligned} &\text{if } V_c \le v^-, \quad Q_{Na} = Q^*_{Na}(v^- - V_c)/v^- \text{ and } Q_K = 0 \\ &\text{if } V_c \ge v^+, \quad Q_K = Q^*_K(V_c - v^+)/v^+ \text{ and } Q_{Na} = 0 \\ &\text{if } V_c \subset (v^-, v^+), \quad Q_K = Q_{Na} = 0 \end{aligned} \qquad (4)$$

where Q^*_{Na} and Q^*_K are characteristic parameters (*Glossary*).

In the absence of cell volume regulatory mechanisms, $Q_K = Q_{Na} = 0$ for any value of V_c.

In the following section, we perform numerical studies of the model employing values corresponding to a typical ideal animal cell. These studies are not exhaustive and are intended only to illustrate some basic properties.

NUMERICAL RESULTS AND DISCUSSION

Numerical methods. To perform the simulations, *Eqs. 1a* and *1b* were integrated numerically, employing the Runge-Kutta fourth-order method, except for the determination of V_m. As mentioned above, after every time step, V_m was calculated assuming *Eq. 1b* by employing a stationary approximation including the electrogenic component (Ref. 22; APPENDIX B). Besides the conditions given by *Eqs. 3* and *4*, a time delay (τ) was introduced in the activation of short-term cell volume regulation. If t is the instant at which V_c reaches the corresponding threshold value, the induced response shall be triggered at $t + \tau$. Time delays have been employed as auxiliary tools for the study of metabolic pathways in the absence of a detailed knowledge of the kinetic properties of the intermediate enzymes (4, 39). For the case of short-term cell volume regulation, the activation of the membrane transporters that determine the regulatory responses requires a complex and incompletely understood chain of intracellular signaling events, mediated by multienzymatic paths [e.g., the phosphatase and kinase cascades (44)]. A time lag ranging from a few seconds to some minutes is to be expected between a perturbation in the concentration of the initial substrate of an enzymatic path and its effect on a final product (14, 15). In concordance with these ideas, we arbitrarily assumed here a τ of 20 s for the activation of short-term cell volume regulation (Table 1), which is characteristic of a relatively fast response. A detailed knowledge of the intermediate enzymes of the signaling paths will permit evaluation of the time delay in terms of the kinetic properties of the enzymes (14, 39).

For the case of osmotic shocks determined by anisosmotic values of Π_e ($[\Pi_e]_{an}$), the extracellular ionic concentrations were corrected according to $([ion]_e)_{an} =$

Table 1. *Numerical values of parameters*

Parameter	Value
A_c	2×10^{-5} cm^2
P_{Na}, P_K, P_{Cl}	10^{-7}, 5×10^{-7}, 10^{-6} cm/s (*cell 1*); 7×10^{-8}, 7×10^{-7}, 10^{-6} cm/s (*cell 2*)
P_w	1.5×10^{-2} cm/s
v^-, v^+	9.99×10^{-9}, 1.001×10^{-8} cm^3
Q^*_{Na}, Q^*_K	0.1, 10 cm$^4\cdot$mol$^{-1}\cdot$s^{-1}
$[Na^+]_e$, $[K^+]_e$, $[Cl^-]_e$, $[X]_e$	1.4×10^{-4}, 10^{-5}, 1.4×10^{-4}, 10^{-5} mol/cm^3
τ	20 s
Π_e	3×10^{-4} mol/cm^3
X_i	1.2×10^{-12} mol (*cell 1*); 1.3×10^{-12} mol (*cell 2*)
N	1.25×10^{-13} mol/cm^2
$[ATP]_i$, $[ADP]_i$, $[P_i]_i$	5×10^{-6}, 6×10^{-8}, 4.95×10^{-6} mol/cm^3
k_{12}	2.5×10^{11} mol$^{-3}\cdot$l$^3\cdot$s^{-1}
k_{23}	10^4 s^{-1}
k_{34}	172 s^{-1}
k_{45}	1.5×10^7 mol$^{-2}\cdot$l$^2\cdot$s^{-1}
$k_{56}°$	2×10^6 mol$^{-1}\cdot$l$\cdot$s^{-1}
k_{61}	1.15×10^4 s^{-1}
k_{21}	10^5 s^{-1}
k_{32}	10^5 mol$^{-1}\cdot$l$\cdot$s^{-1}
k_{43}	1.72×10^4 mol$^{-3}\cdot$l$^3\cdot$s^{-1} *
k_{54}	2×10^5 mol$^{-1}\cdot$l$\cdot$s^{-1}
$k_{65}°$	30 s^{-1}
k_{16}	6×10^8 mol$^{-2}\cdot$l$^2\cdot$s^{-1}
K_{eq}	239,000 mol/l

*Although numerical values for rate constants employed for calculations in Ref. 22 and in the present work were those of Chapman et al. (10), reproduced here, the reader must be aware that an error was introduced in Table 1 of Ref. 22 in value and units of k_{43}. See *Glossary* for definition of the abbreviations.

r[ion]$_e$, where r = $(\Pi_e)_{an}/\Pi_e$. The osmotic shocks were thus determined not solely by the modification of the ambient concentration of a nontransported ("inert") solute, but via modifications of the concentrations of all the extracellular ionic species.

For the particular conditions, the steady-state values of the variables were initially obtained from the corresponding time integrations and confirmed by an iterative procedure (APPENDIX C). The dependent variables were plotted as the absolute values of V_m, V_c, and the corresponding ionic concentrations ($[Na^+]_i = m_{Na}/V_c$, $[K^+]_i = m_K/V_c$, and $[Cl^-]_i = m_{Cl}/V_c$). In every run, the following control tests were performed to guarantee the physicochemical consistency of the simulation. *1*) Once a steady state is achieved, the conditions of osmotic equilibrium and of macroscopic electroneutrality must be simultaneously satisfied

$$(X_i + m_{Na} + m_K + m_{Cl})/V_c = \Pi_e$$
$$(X_i + m_{Cl}) = (m_{Na} + m_K) \quad (5a)$$

2) In the absence of volume-induced regulatory fluxes (that is, for $\phi_{Na} = \phi_K = 0$), the steady-state values of m_{Cl}, V_c, and V_m must satisfy the Nernst equilibrium for Cl^-

$$m_{Cl}/V_c = [Cl^-]_e \exp(FV_m/RT) \quad (5b)$$

Reference state. We determined reference states for two different cases (*cell 1* and *cell 2*, Table 1). *Cell 1* contains a smaller amount of the fixed anion (and, as a consequence, a larger amount of intracellular Cl^- in the reference state; see below) than *cell 2*. Unless otherwise specified, the numerical values of the parameters employed for the simulations were those shown in Table 1. Among these values, the osmotic permeability (P_w) corresponds to that determined for several animal cells (for references, see Ref. 57). The basal ionic permeabilities (P_{Na}, P_K, and P_{Cl}) are also within the corresponding experimental ranges (e.g., see Ref. 54). As can be seen, both *cell 1* and *cell 2* are characterized by relatively large P_K and P_{Cl} and by a lesser P_{Na}. The total amount of impermeant solute (X_i) is a reasonable estimate for a cell with an average volume of 10^{-8} cm^3 (29). The extracellular ionic concentrations ($[Na^+]_e$, $[K^+]_e$, $[Cl^-]_e$, and $[X]_e$) were arbitrarily fixed and approximately correspond to the usual isotonic extracellular values (54) under physiological conditions. Because Cl^- is the only diffusible anion considered in the model, its extracellular concentration was set slightly higher than the usual physiological value, to compensate for other diffusible anions. The density of Na^+-K^+-ATPase (N) falls within the physiological range (10, 18, 22), as also do the $[ATP]_i$, $[ADP]_i$, and $[P_i]_i$ (32). The equilibrium constant (K_{eq}) is characteristic of the ATP hydrolysis (32). The rate constants of the enzymatic reaction were taken from Chapman et al. (10). The values chosen for the threshold cell volumes are arbitrary and characteristic of a highly sensitive cell; actual control values could correspond to an ~1–5% change in the reference volume of the cell (26, 46). In this respect, studies performed with threshold values corresponding to a less sensitive cell reveal behaviors basically similar to the ones shown here, except that the volume recovery after anisosmotic shocks occur (with close approximation) not to the initial reference values but to the threshold ones (e.g., see Fig. 10). The other parameters of the model were heuristically determined by a trial-and-error method, to obtain a plausible behavior of the model. For the parameter values listed in Table 1, the reference values of the variables satisfy the steady state under the isotonic condition ($\Pi_e = 3.0 \times 10^{-4}$ mol/cm^3).

The reference values of variables for *cell 1* were $V_c(0)$, 1×10^{-8} cm^3; $V_m(0)$, -4.1×10^{-2} V; $[Na^+]_i(0)$, 1.84×10^{-5} mol/cm^3; $[K^+]_i(0)$, 1.32×10^{-4} mol/cm^3; and $[Cl^-]_i(0)$, 3.02×10^{-5} mol/cm^3.

For *cell 2*, they were $V_c(0)$, 1×10^{-8} cm^3; $V_m(0)$, -5.2×10^{-2} V; $[Na^+]_i(0)$, 1.65×10^{-5} mol/cm^3; $[K^+]_i(0)$, 1.33×10^{-4} mol/cm^3; and $[Cl^-]_i(0)$, 2.01×10^{-5} mol/cm^3.

Because the study is mainly illustrative, these values do not correspond to any specific cell type. For a roughly spherical cell, a V_c of 10^{-8} cm^3 would approximately correspond to a cell diameter of 25 μm. Together with the rest of the values corresponding to the reference states and parameters (Table 1), these values could approximately characterize, for instance, some cells of the hematopoietic lines, like large lymphocytes or granulocytes (27, 51, 52).

Effect of Na^+-K^+-ATPase on the reference state. Figure 3, *A* and *B*, shows the dependence of the cell steady state on N, for a physiological range (18) and for the

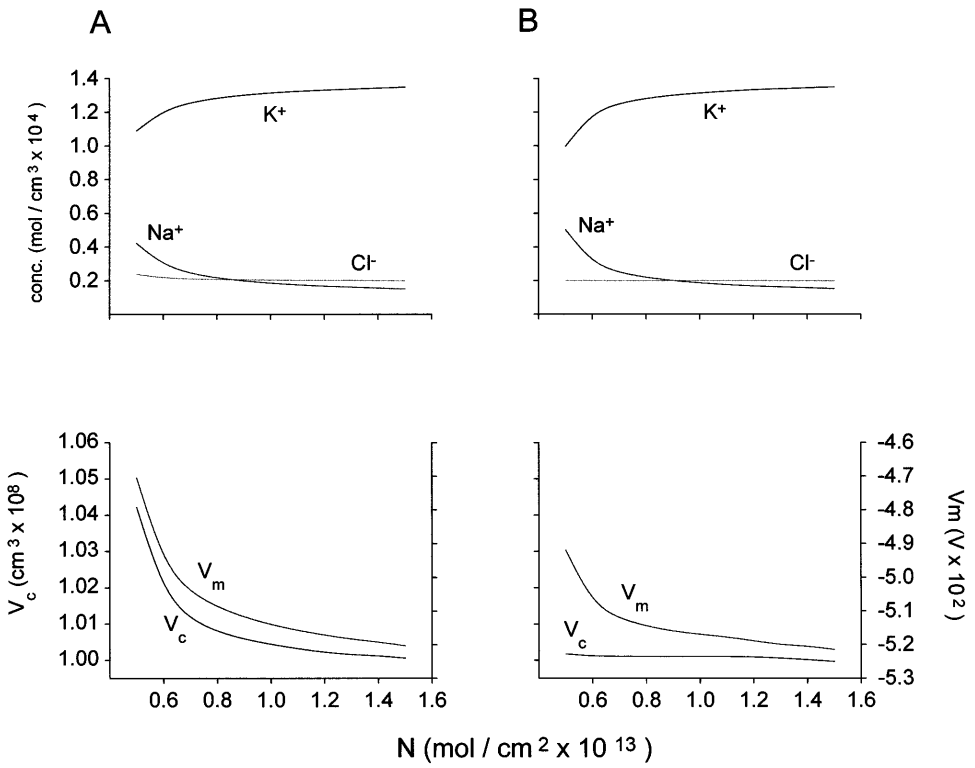

Fig. 3. Plots of steady-state values of intracellular concentrations of Na^+, K^+, and Cl^- ($[Na^+]_i$, $[K^+]_i$, and $[Cl^-]_i$) and of cell volume (V_c) and electrical potential difference across the cell membrane (V_m) vs. total Na^+-K^+-ATPase membrane density (N) under nonregulatory (A) and regulatory (B) conditions, for case of *cell 2*.

case of *cell 2*. To obtain the final steady-state values, the model was run employing the reference state as the initial state and subject to the perturbation determined by the particular value chosen for N. As mentioned, the values obtained were then employed as the inputs of an iterative procedure to determine the roots (APPENDIX C). In every case, this procedure confirmed that the system had indeed reached the steady state after the time run. Typically, the system achieved the steady state at ~2,000 s. For lower values of N, the behavior of the system was not significantly different from the one corresponding to the complete inhibition of the enzyme (see below).

For the interval considered, and in the absence of short-term cell volume regulation (Fig. 3*A*), $[K^+]_i$ increases and $[Na^+]_i$ decreases with N. There is a small variation in V_m, since its steady-state value is basically given by the electrodiffusive component. For this reason and also due to the fact that in the absence of cell volume regulatory mechanisms $[Cl^-]_i$ is determined by electrochemical equilibrium, there is a negligible variation of $[Cl^-]_i$ with N. As expected, V_c increases with decreasing N, since fewer diffusible cations are being extruded from the cell. Although the global final effects are basically similar, the variation of N in the presence of short-term cell volume regulation (Fig. 3*B*) determines some distinctive features. Because V_c increases with decreasing N, the mechanisms for RVD are activated. The additional net efflux of KCl induced by this activation produces a larger decrease of $[K^+]_i$ than in the nonregulatory case and compensates for the increase in $[Na^+]_i$. For the interval of values of N considered, the regulatory mechanisms succeed in maintaining V_c at the reference value, despite a significant diminution of the enzyme density.

Effect of Na^+-K^+-ATPase inhibition under isotonic conditions. The effect of the complete inhibition of the Na^+ pump on the time-dependent behavior is shown in Fig. 4, *A* and *B*, for the case of *cell 2*. In the absence of short-term cell volume regulation (Fig. 4*A*), the pump inhibition immediately produces the expected consequences: a decrease in $[K^+]_i$, an increase in $[Na^+]_i$ and $[Cl^-]_i$, and an increase in V_c and membrane depolarization. These results are consistent with classic experimental evidence (8) and with previous model simulations employing phenomenological formulations of the enzyme (29). In the presence of active mechanisms of short-term cell volume regulation (Fig. 4*B*), the cell is capable of maintaining V_c at the reference value until $[K^+]_i$ becomes sufficiently low. At this instant, the regulatory flux of KCl turns from efflux into influx, $[Cl^-]_i$ starts to increase, and the fall of $[K^+]_i$ becomes less steep. These results could provide a means to interpret controversial evidence of cells in which the pump inhibition does not produce an immediate increase in cell volume (3, 30, 36). As for the nonregulatory case, however, the cell finally evolves toward a Gibbs-Donnan equilibrium (see above). In both plots, the initial abrupt depolarization step exhibited by the V_m curves (see also below) corresponds to the sudden inhibition of the electrogenic component of the enzyme.

Restitution of the pump to its normal physiological density produces a complete recovery of the cell to its reference steady state. In Fig. 5, we show the recovery of *cell 2* in the presence of short-term cell volume regulation. In particular, V_m gradually becomes more electronegative. The initial abrupt hyperpolarization exhibited by the V_m curve corresponds to the sudden turning on of the electrogenic component.

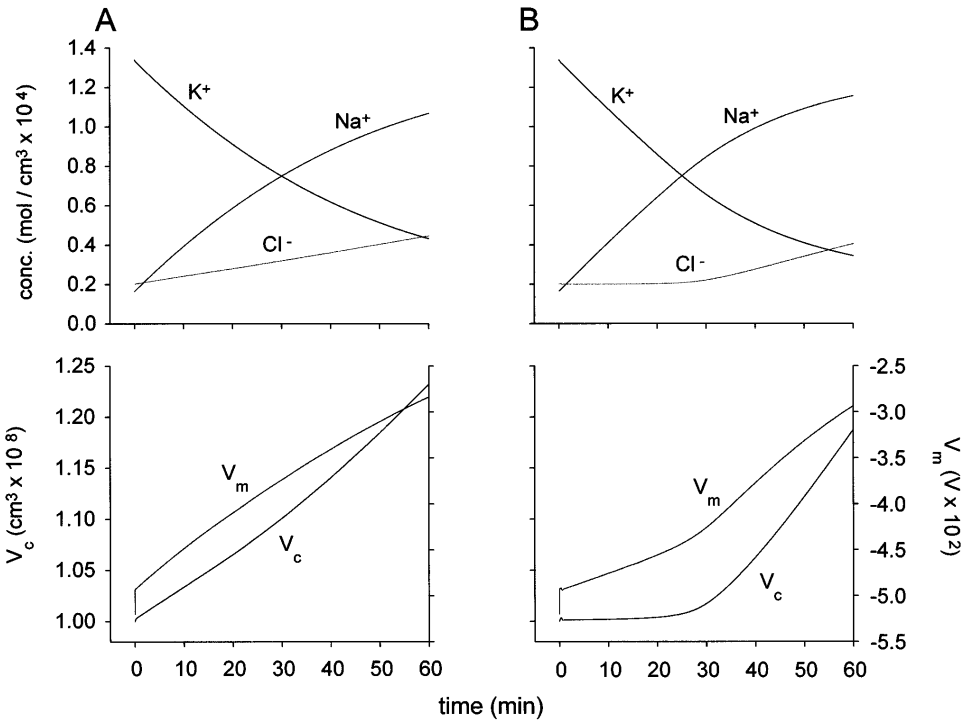

Fig. 4. *A*: dynamic response of *cell 2* to a complete inhibition of Na^+ pump ($N = 0$), for nonregulatory case. $[Na^+]_i$, $[K^+]_i$, $[Cl^-]_i$, V_c, and V_m are plotted as functions of time. Initial state: reference state. *B*: analogous to *A*, but for regulatory condition.

Responses to anisosmotic shocks. Figures 6 and 7 show the time course of the changes induced by anisosmotic shocks, as obtained from the simulation of *cell 1* subject to hypotonic (Fig. 6) and hypertonic (Fig. 7) perturbations of the extracellular medium. In the presence of volume regulatory mechanisms, *cell 1* exhibits the typical dynamic responses corresponding to RVD (Fig. 6) and RVI (Fig. 7) (5, 20). When RVD is triggered (Fig. 6*A*), both $[K^+]_i$ and $[Cl^-]_i$ decrease; however, while $[K^+]_i$ is restored by the pump activity, $[Cl^-]_i$ remains at lower values. V_m becomes more electronegative, as a consequence of the fall in $[Cl^-]_i$ and of the rather large Cl^- permeability. After the transient phase of the regulatory response, V_c recovers to its reference value. Throughout the response, $[Na^+]_i$ remains approximately constant. When RVI is triggered (Fig. 7*A*), both $[Na^+]_i$ and $[Cl^-]_i$ increase. V_m becomes more electropositive, as a consequence of the increase in $[Cl^-]_i$. Correspondingly, $[K^+]_i$ experiences a slight fall. In the case shown, V_c recovers to its reference value. In Figs. 6*B* and 7*B*, one will notice that the acute phase of short-term cell volume regulation is not affected by the inhibition of the Na^+ pump. However, once the acute phase is over, the long-term effects described above for the case of complete pump inhibition become noticeable (e.g., V_c slowly increases; other effects not shown). Also, a concomitant activation (within physiological values) of the Na^+ pump did not produce any effect on the short-term regulatory response (not shown), either for RVD or for RVI. Figures 6*B* and 7*B* also include the osmometer behavior of cells in the absence of regulatory mechanisms, when an increased (decreased) steady-state V_c results from exposure to a hypotonic (hypertonic) medium.

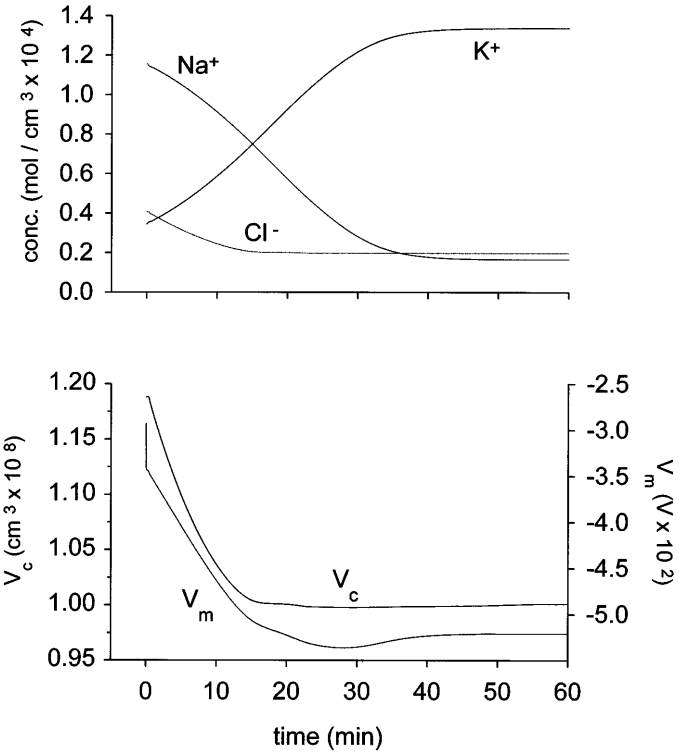

Fig. 5. Recovery of *cell 2* after inhibition of Na^+ pump, for regulatory case. Initial state: $[Na^+]_i$, $[K^+]_i$, $[Cl^-]_i$, V_c, and V_m after 3,800 s of complete pump inhibition (see Fig. 4). N corresponded to physiological value (Table 1). $[Na^+]_i$, $[K^+]_i$, $[Cl^-]_i$ (*top*), V_c, and V_m (*bottom*) are plotted as functions of time.

Figures 8 and 9 show the temporal responses of *cell 1* (Figs. 8*A* and 9*A*) and *cell 2* (Figs. 8*B* and 9*B*) to anisosmotic shocks, for different ambient osmolarities. For the case of hyposmotic shocks, both *cell 1* (Fig. 8*A*) and *cell 2* (Fig. 8*B*) are incapable of eliciting an appropriate RVD response at sufficiently low osmolarities. Because, in this case, *cell 1* nevertheless exhibits a

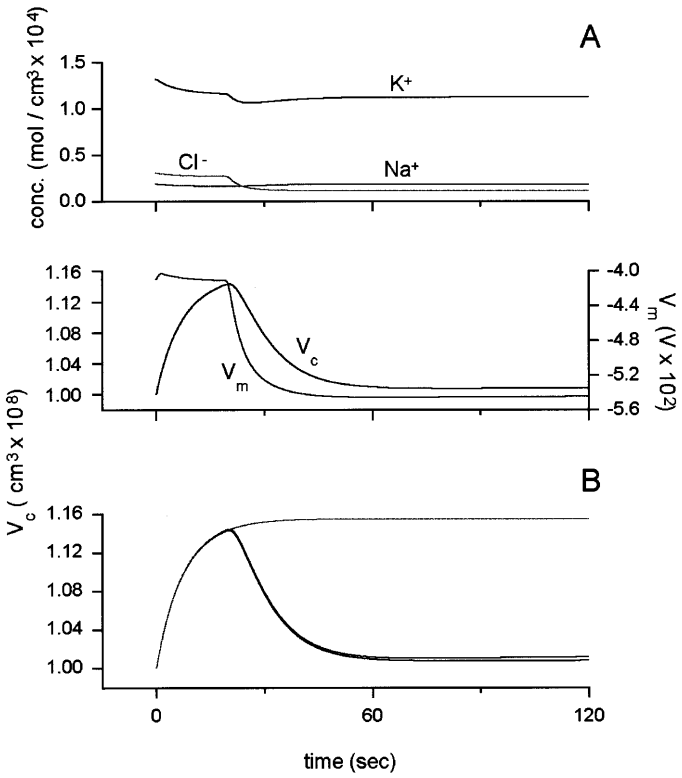

Fig. 6. Response of *cell 1* to a hyposmotic shock ($\Pi_e = 2.6 \times 10^{-4}$ mol/cm^3). Initial state: reference state. *A*: plots of $[Na^+]_i$, $[K^+]_i$, $[Cl^-]_i$ (*top traces*), V_c, and V_m (*bottom traces*) as functions of time, during regulatory response. *B*: plots of V_c as a function of time for 3 cases: *1*) under nonregulatory conditions (osmometric curve), *2*) under regulatory conditions and physiological *N* [regulatory volume decrease (RVD) curve], and *3*) under regulatory conditions and complete pump inhibition ($N = 0$; superposed RVD curve).

better capability than *cell 2*, we can relate these partial responses to an insufficient availability of intracellular Cl^-. Similar conclusions have been obtained from studies of previous models of cell volume regulation mediated by Cl^- permeability changes (55). Because both Na^+ and Cl^- are present at large extracellular concentrations, neither *cell 1* (Fig. 9*A*) nor *cell 2* (Fig. 9*B*) exhibits limits to the capability to perform RVI. From these results, cell volume regulatory responses by which the initial reference value is not completely restored might occur by two different mechanisms: *1*) with threshold values for the regulatory response that are significantly different from the reference V_c (for both RVD and RVI; see also *Reference state* and Fig. 10) or *2*) with partial intracellular Cl^- availability (for RVD, in cells in which this response is mediated by volume-induced KCl efflux). It has been suggested that incomplete cell volume recovery from short-term regulation could play a role in cellular adaptation (21).

Figure 10 shows the temporal responses of *cell 1* to anisosmotic shocks for different values of v^- and v^+ and of the kinetic parameters of the cell volume-induced fluxes (Q^*_{Na} and Q^*_K). As expected, the regulatory responses depend critically on the magnitude of the kinetic parameters of the cotransport systems (Fig. 10, *A* and *B*). As can also be seen, the regulatory response drives the V_c toward the corresponding threshold value (Fig. 10, *C* and *D*).

In Fig. 11, we show the recovery of *cell 1* to anisosmotic shocks in the presence of short-term cell volume regulation. As can be seen, restitution of the ambient osmolarity to the normal physiological value results in a complete recovery of the cell to its reference steady state. In the case of a complete inhibition of the Na^+ pump (not shown), the cell cannot recover from an anisosmotic shock, and evolves in a fashion similar to the isotonic case (see above). Notice that the RVD response under recovery conditions (Fig. 11*A*) is steeper than the one elicited by a hyposmotic shock (Fig. 6). This is basically due to the fact that, for the recovery process, the initial $[Cl^-]_i$ is significantly larger than in the case of the hyposmotic shock. This more intense response determines a transit across the threshold cell volume values (manifested by the "undershoot" in Fig. 11*A*, *bottom*) and the consequent activation of the RVI response after the corresponding time delay.

Activation of Na^+-K^+-ATPase under isotonic conditions. In the long term, modification of *N* within the physiological range does not determine significant changes in V_m (Fig. 3). For those values of *N*, the overall steady-state contribution of the enzyme to the membrane depolarization is therefore small, mainly as a consequence of the dominant diffusive component. The

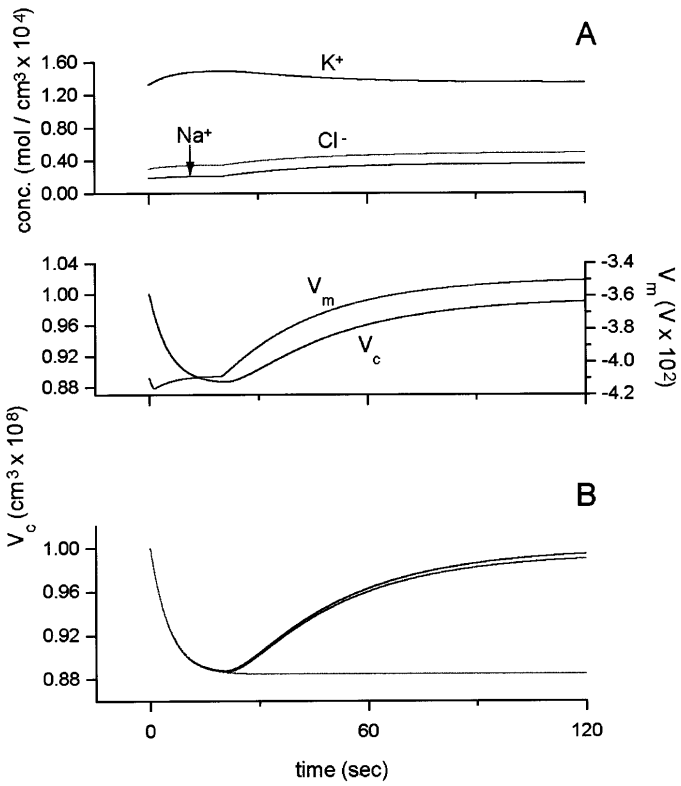

Fig. 7. Similar to Fig. 6, but for a hyperosmotic shock ($\Pi_e = 3.4 \times 10^{-4}$ mol/cm^3). *A*: plots of $[Na^+]_i$, $[K^+]_i$, $[Cl^-]_i$ (*top traces*), V_c, and V_m (*bottom traces*) as functions of time, during regulatory response. *B*: plots of V_c as a function of time for 3 cases: *1*) under nonregulatory conditions (osmometric curve), *2*) under regulatory conditions and physiological *N* [regulatory volume increase (RVI) curve], and *3*) under regulatory conditions and complete pump inhibition ($N = 0$; superposed RVI curve).

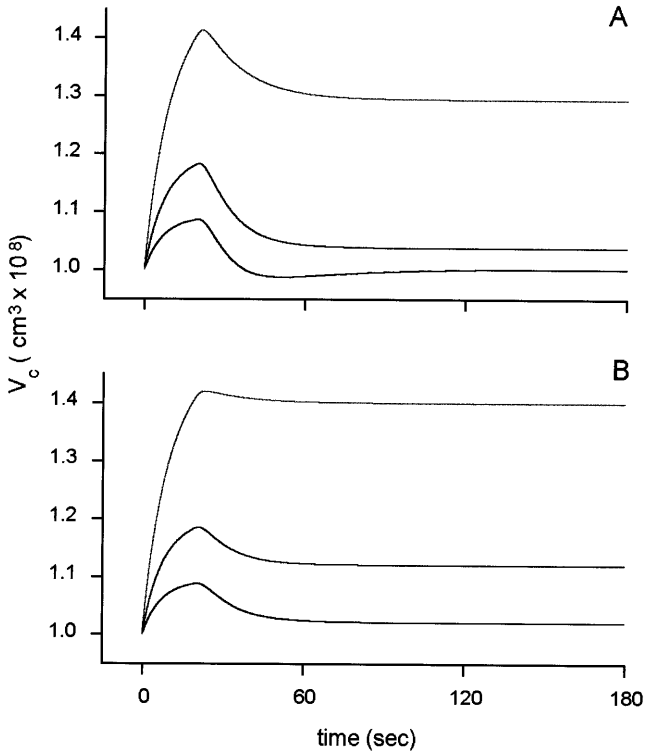

Fig. 8. Responses of *cell 1* (*A*) and *cell 2* (*B*) to hyposmotic shocks of increasing hypotonicity (from *bottom* to *top* in both *A* and *B*: Π_e = 2.75×10^{-4}, 2.5×10^{-4}, and 2.0×10^{-4} mol/cm^3).

cellular response to the activation of the enzyme can be examined more closely in the time-dependent behavior, during the initial phases after the perturbations. In Fig. 12, we show the effects of pump activation under nonregulatory (Fig. 12*A*) and regulatory (Fig. 12*B*) conditions of cell volume. For both the nonregulatory and regulatory cases, after the initial abrupt change toward hyperpolarization, V_m undergoes relaxation to the reference state. Throughout the simulation, V_c and the ionic concentrations experience slight modifications. $[Na^+]_i$ decreases and $[K^+]_i$ increases slowly in response to enzyme activation; $[Cl^-]_i$ remains basically unchanged. In particular, Fig. 12*B* reveals the sudden (although small) change in V_c and V_m determined by the activation of the mechanisms of cell volume regulation.

The inactivation of the Na^+ pump abruptly drives V_m toward the diffusive membrane potential (see initial phase in Fig. 4, *A* and *B*). V_m afterwards experiences the slow depolarization associated with the long-term ionic concentration changes determined by the pump inhibition. Similar results can be obtained by dramatic decreases in $[ATP]_i$ (not shown). The abrupt initial change in V_m in response to enzyme inhibition (or, equivalently, to ATP depletion) is consistent with experimental evidence about the electrogenic contribution of the Na^+ pump to the membrane potential (13). This response can be interpreted in electrical terms as the sudden shutting off of an electric current source (1). Analogously, the abrupt hyperpolarizing response to enzyme activation (Fig. 12) can be interpreted as the sudden turning on of the current source associated with the electrogenic component. As can be seen in Fig. 12, this electrogenic ionic current is sufficient to determine macroscopic electrical effects of short duration (in the form of the transient modification of V_m) but does not contribute to significant changes in the ionic concentrations or in the V_c. For the physiological values of N, the physicochemical conditions imposed by the overall dynamic model (e.g., tendency to simultaneously achieve macroscopic electroneutrality and isotonic equilibrium, high Cl^- and K^+ permeabilities, and so forth) afterwards forces the relaxation of V_m to values similar to that corresponding to the reference state.

Taken together, the changes in N and $[ATP]_i$ determine both short- and long-term effects. The short-term effects (Figs. 4 and 12) depend on modifications of the electrogenic component of the Na^+ pump and consist of electrical signals of short duration. Within certain intervals of N and $[ATP]_i$ values, no significant long-term modifications (e.g., of the ionic concentrations and consequently of the V_c and membrane potential) take place (Figs. 3, 4, and 12). However, the same changes in enzyme activity would determine a significant short-duration signal. If they took place in actual cells, the short-term electrical signals triggered in response to a slight activation of the enzyme (Fig. 12) might play a role in intra- or intercellular signaling (43). Thus the activation of the electrogenic component might, for instance, mediate fast cellular responses to effectors that would act via the Na^+ pump, like certain hormones (for references, see Ref. 21).

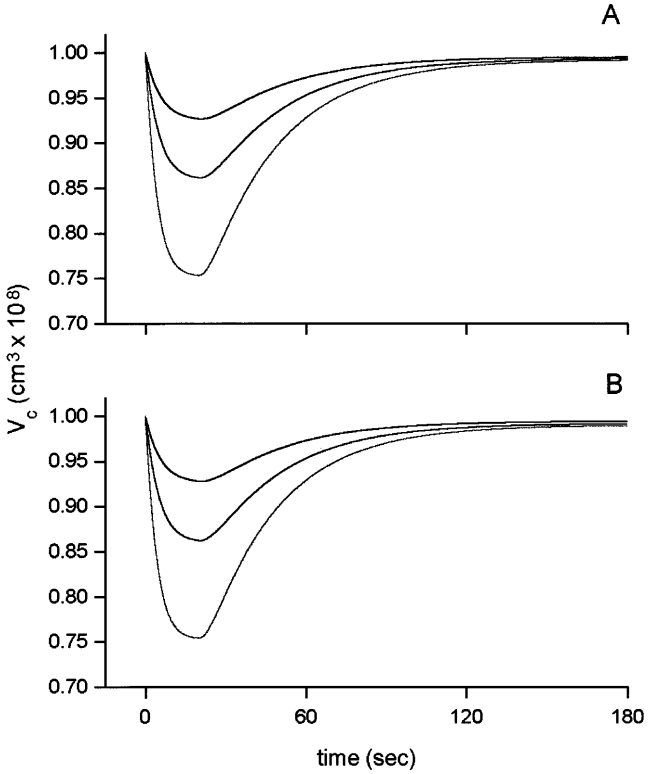

Fig. 9. Responses of *cell 1* (*A*) and *cell 2* (*B*) to hyperosmotic shocks of increasing hypertonicity (from *top* to *bottom* in both *A* and *B*: Π_e = 3.25×10^{-4}, 3.5×10^{-4}, and 4.0×10^{-4} mol/cm^3).

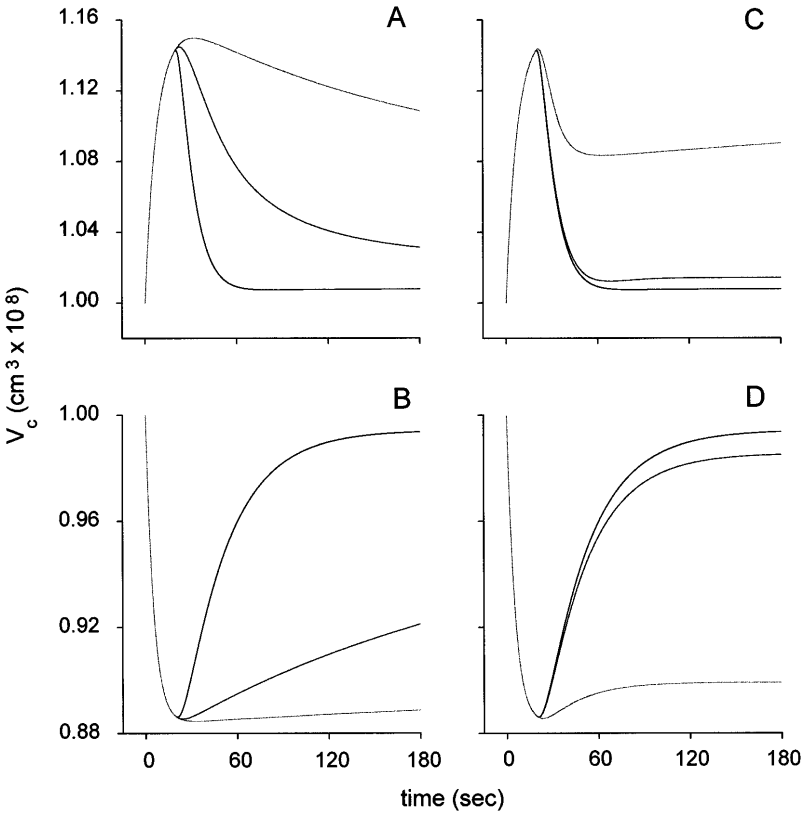

Fig. 10. Responses of *cell 1* to hyposmotic shocks (*A* and *C*; $\Pi_e = 2.6 \times 10^{-4}$ mol/cm^3) and hyperosmotic shocks (*B* and *D*; $\Pi_e = 3.4 \times 10^{-4}$ mol/cm^3) for different threshold values of cell volume (v^-, v^+) and kinetic parameters of cell volume-induced fluxes (Q^*_{Na} and Q^*_K). Initial state: reference state. From *top* to *bottom*: $Q^*_K = 0.1$, 1, and 10 cm$^4 \cdot$mol$^{-2} \cdot$s^{-1} (*A*); $Q^*_{Na} = 0.1$, 0.01, and 0.001 cm$^4 \cdot$mol$^{-2} \cdot$s^{-1} (*B*); v^- and $v^+ = 9 \times 10^{-9}$ and 1.1×10^{-8}, 9.9×10^{-9} and 1.01×10^{-8}, and 9.99×10^{-9} and 1.001×10^{-8} cm^3 (*C*); and v^- and $v^+ = 9.99 \times 10^{-9}$ and 1.001×10^{-8}, 9.9×10^{-9} and 1.01×10^{-8}, and 9×10^{-9} and 1.1×10^{-8} cm^3 (*D*).

In conclusion, the model consistently describes properties associated with the long-term role of Na^+-K^+-ATPase. For the physiological range of Na^+-K^+-ATPase densities, the reference state of the cell depends on whether the volume regulatory mechanisms are present or not. In particular, in the absence of short-term cell volume regulation, the cell volume increases when the enzyme density decreases, since a gradually declining number of diffusible cations is extruded from the cell. In the presence of an active mechanism of short-

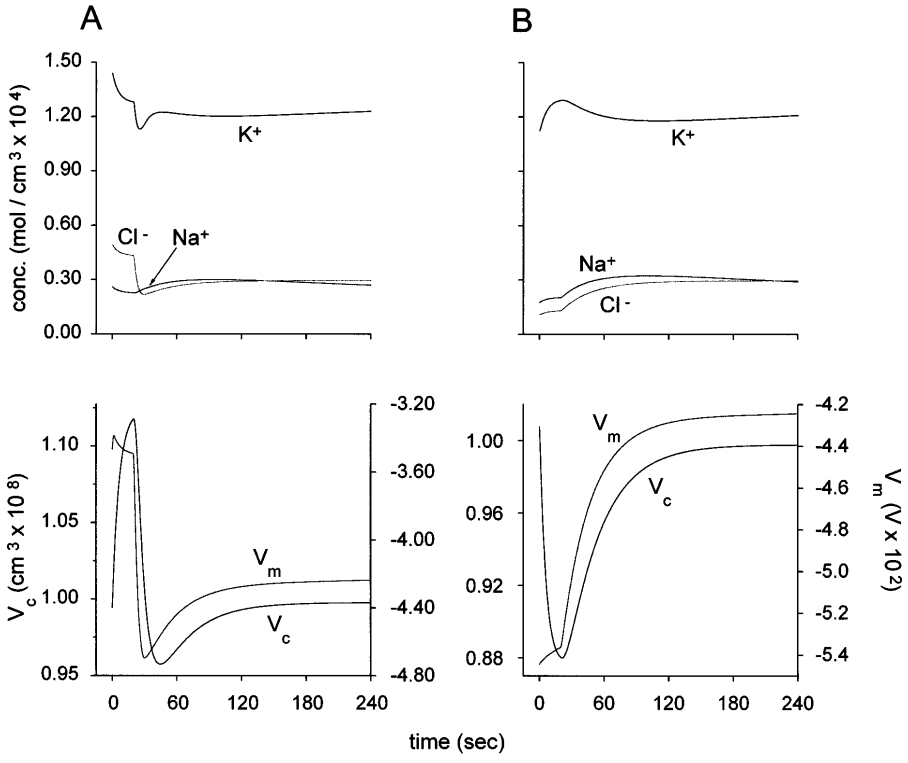

Fig. 11. *A*: recovery of *cell 1* from a hyperosmotic shock. Initial state: $[Na^+]_i$, $[K^+]_i$, $[Cl^-]_i$, V_c, and V_m after 2,000 s of run after a hyperosmotic shock ($\Pi_e = 3.4 \times 10^{-4}$ mol/cm^3; see Fig. 7). For run, Π_e was set at 3×10^{-4} mol/cm^3 (isotonic). *B*: similar to *A*, but depicting recovery from a hyposmotic shock (Fig. 6).

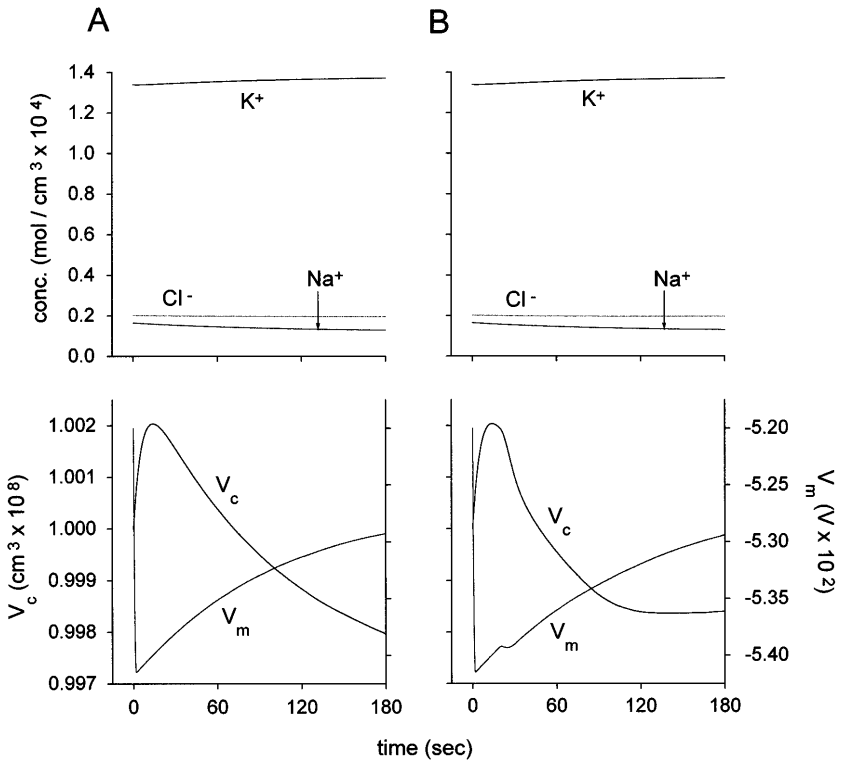

Fig. 12. Na^+-K^+-ATPase activation ($N = 2.5 \times 10^{-13}$ mol/cm^2) for *cell 2* under nonregulatory (*A*) and regulatory (*B*) conditions. Initial state: reference state.

term cell volume regulation, and for the interval considered, the cell is capable of maintaining its volume despite a decrease in the enzyme density. Some authors suggest that, to assure proper macromolecular activity, it is critical that the value of the cell volume be kept within a narrow interval. If this is the case, our results suggest that the permanent triggering of acute volume regulatory mechanisms might also play a role in chronic cell homeostasis, by contributing to the maintenance of the cell volume in the event of a partial inactivation of the Na^+ pump. In the time-dependent behavior, the complete inhibition of the enzyme reproduces the classic experimental results (decrease in $[K^+]_i$ and in V_c, increase in $[Na^+]_i$ and $[Cl^-]_i$, and membrane depolarization). In the presence of regulatory mechanisms, the cell is capable of maintaining its volume at the reference value until $[Cl^-]_i$ becomes sufficiently low.

The model introduced here represents a plausible description of the short-term responses of a schematic cell to anisosmotic shocks. In the absence of cell volume regulation, the model describes the osmometer behavior. In the presence of active mechanisms of volume regulation, the model consistently describes both RVD and RVI. In the present work, these responses are achieved via the activation of ionic cotransport systems that remain inactive under reference conditions and are activated by minute cell volume changes. These short-term responses exhibit a negligible dependence on the enzyme parameters. The variation of N and $[ATP]_i$ both have undetectable effects on RVD and RVI, although they affect the cell recovery. From a biological point of view, this would imply that the acute regulatory responses are not significantly affected by the pump condition. This is consistent with the view that an enzyme of the Na^+-K^+-ATPase type mainly plays a long-term role in the generation of electrochemical gradients. However, the preexistence of these gradients is crucial for the short-term responses. The simulations performed here also suggest that partial or incomplete RVD responses might be related to insufficient intracellular Cl^- availability.

The method introduced here to calculate V_m underlies the characteristic time-dependent behaviors of the model. If the method turns out to be an appropriate approximation, the model predicts short-term electrical responses to the Na^+ pump activation, which are a consequence of the electrogenic properties of the enzyme. Because the enzyme is a target of diverse effectors of cellular responses, we suggest that these short-duration electrical signals might be involved in signaling mechanisms.

APPENDIX A

Steady-State Analysis of Na^+-K^+-ATPase Kinetic Model

The active transport of Na^+ and K^+, mediated by Na^+-K^+-ATPase, is described by the state diagram shown in Fig. 2. In this diagram, $N_1, \cdots, N_6$ are the intermediate states of the enzyme, and $k_{12}, \cdots, k_{61}$ and $k_{16}, \cdots, k_{21}$ are the rate constants governing the corresponding transitions in the clockwise and counterclockwise directions, respectively. The meanings of the rest of the symbols are specified in the *Glossary*. The steady-state analysis of this diagram has already been performed (10, 22, 34); we show here the main expressions. In the steady state, the cycle flux J_p (considered to be positive in the clockwise direction) can be expressed, employing the diagram method (23), as

$$J_p = (1/\Sigma)(\alpha - \beta) \qquad (A1)$$

In this equation, α and β are functions, defined as

$$\alpha = N a_{12} a_{23} a_{34} a_{45} a_{56} a_{61}$$
$$\beta = N a_{21} a_{32} a_{43} a_{54} a_{65} a_{16} \quad (A2)$$

with

$$a_{12} = k_{12} (m_{Na/V_c})^3 \qquad a_{21} = k_{21}$$
$$a_{23} = k_{23} \qquad a_{32} = k_{32} [ADP]_i$$
$$a_{34} = k_{34} \qquad a_{43} = k_{43} [Na^+]_e^3$$
$$a_{45} = k_{45} [K^+]_e^2 \qquad a_{54} = k_{54} [P_i]_i$$
$$a_{56} = k_{56} [ATP]_i \qquad a_{65} = k_{65}$$
$$a_{61} = k_{61} \qquad a_{16} = k_{16} (m_k/V_c)^2$$

and Σ is the sum of all the directional diagrams of the model and is therefore a function of all the rate constants and ligand concentrations (see Ref. 22 for explicit expression).

The rate constants k_{56} and k_{65} are assumed to depend on V_m according to

$$k_{56} = k_{56}^\circ \exp(FV_m/2RT)$$
$$k_{65} = k_{65}^\circ \exp(-FV_m/2RT) \quad (A3)$$

where k_{56}° and k_{65}° are independent of V_m.

The detailed balance condition imposes the following restriction on the rate constants

$$K_{eq} = \frac{k_{12}\, k_{23}\, k_{34}\, k_{45}\, k_{56}^\circ\, k_{61}}{k_{65}^\circ\, k_{54}\, k_{43}\, k_{32}\, k_{21}\, k_{16}} \quad (A4)$$

where K_{eq} is the equilibrium constant of the reaction ATP + $H_2O \leftrightarrow$ ADP + P_i.

Because there is only one cycle, the active fluxes of Na^+ and K^+ (considered to be positive in the inward direction) are respectively equal to $-3J_p$ and $2J_p$.

APPENDIX B

Stationary Solution for V_m

After each integration time step, we determined V_m, assuming *Eq. 1b*, as a solution of the transcendental equation (22)

$$V_m = (RT/F) \ln [(\kappa + \lambda)/(\mu + \omega)] \quad (B1)$$

where the functions $\kappa = \kappa(V_m)$, $\lambda = \lambda(V_m)$, $\mu = \mu(V_m)$, and $\omega = \omega(V_m)$ are given by

$$\kappa = \{P_{Na} [Na^+]_e + P_K [K^+]_e + P_{Cl} (m_{Cl}/V_c)\} \epsilon_m$$
$$\lambda = (N/\Sigma) a_{21}\, a_{32}\, a_{43}\, a_{54}\, a_{65}^\circ\, a_{16}$$
$$\mu = \{P_{Na} (m_{Na}/V_c) + P_K (m_K/V_c) + P_{Cl} [Cl^-]_e\} \epsilon_m$$
$$\omega = (N/\Sigma) a_{12}\, a_{23}\, a_{34}\, a_{45}\, a_{56}^\circ\, a_{61}$$

with ϵ_m defined by *Eqs. 2*, Σ and the a_{ij} terms defined in APPENDIX A, and a_{56}° and a_{65}° given by

$$a_{56}^\circ = k_{56}^\circ [ATP]_i$$
$$a_{65}^\circ = k_{65}^\circ$$

It must be noted that Σ is also a function of V_m (see APPENDIX A).

V_m was determined from *Eq. B1* by an iteration of the type $(V_m)_{n+1} = f(V_m)_n$, which yielded convergent solutions for all the simulations. In the absence of electrogenic transport (e.g., for $N = 0$), *Eq. B1* becomes the Goldman-Hodgkin-Katz (17, 24) explicit equation for the diffusion potential

$$(V_m)_{diff} = (RT/F) \ln(\kappa/\mu) \quad (B2)$$

APPENDIX C

Determination of Steady-State Values

In the steady state, *Eqs. 1a* satisfy

$$dm_{Na}/dt = dm_K/dt = dm_{Cl}/dt = dV_c/dt = 0 \quad (C1)$$

From *Eqs. 1b* and *C1*, we can express the steady-state values of the variables by the following system of equations

$$m_{Na} = [Na^+]_e \exp(-u) V_c + [\exp(-u/2) V_c/P_{Na} \epsilon_m] (-3J_p + \phi_{Na}) = f_1(m_{Na}, m_K, m_{Cl}, V_c, V_m)$$
$$m_K = [K^+]_e \exp(-u) V_c + [\exp(-u/2) V_c/P_K \epsilon_m] (2J_p + \phi_K) = f_2(m_{Na}, m_K, m_{Cl}, V_c, V_m)$$
$$m_{Cl} = [Cl^-]_e \exp(u) V_c + [\exp(u/2) V_c/P_{Cl} \epsilon_m] (\phi_{Na} + \phi_K) = f_3(m_{Na}, m_K, m_{Cl}, V_c, V_m)$$
$$V_c = (X_i + m_{Na} + m_K + m_{Cl})/\Pi_e = f_4 m_{Na}, m_K, m_{Cl}, V_c, V_m)$$
$$V_m = (RT/F) \ln[(\kappa + \lambda)/(\mu + \omega)] = f_5(m_{Na}, m_K, m_{Cl}, V_c, V_m) \quad (C2)$$

where the last equation is actually *Eq. B1* (see above for the meaning of the symbols).

Similar to the procedure described in APPENDIX B, the roots of *Eqs. C2* were determined by an iteration of the type $(y)_{n+1} = f_i(m_{Na}, m_K, m_{Cl}, V_c, V_m)_n$ ($y = m_{Na}, m_K, m_{Cl}, V_c, V_m$; $i = 1, 2, \cdots, 5$), which yielded convergent solutions for all the simulations.

This work was supported by grants from the Programa para el Desarrollo de las Ciencias Básicas and from the Comisión Intersectorial de Investigación Científica de la Universidad de la República, Uruguay.

A preliminary version of this work was presented at the III Congreso Iberoamericano de Biofísica, held at Buenos Aires, Argentina, in September 1997.

Address for reprint requests: J. A. Hernández, Sección Biofísica, Facultad de Ciencias, Iguá s/n, esq. Mataojo, 11400 Montevideo, Uruguay.

Received 3 November 1997; accepted in final form 11 June 1998.

REFERENCES

1. **Abercrombie, R. F., and P. De Weer.** Electric current generated by squid giant axon sodium pump: external K and internal ADP effects. *Am. J. Physiol.* 235 (*Cell Physiol.* 4): C63–C68, 1978.
2. **Adorante, J. S., and P. M. Cala.** Mechanisms of regulatory volume decrease in nonpigmented human ciliary epithelial cells. *Am. J. Physiol.* 268 (*Cell Physiol.* 37): C721–C731, 1995.
3. **Alvarez-Leefmans, F. J., S. M. Gamiño, and L. Reuss.** Cell volume changes upon sodium pump inhibition in *Helix aspersa* neurons. *J. Physiol. (Lond.)* 458: 603–619, 1992.
4. **Van der Heiden, U.** Delays in physiological systems. *J. Math. Biol.* 8: 345–364, 1979.

5. **Baumgarten, C. M., and J. J. Feher.** Osmosis and the regulation of the cell volume. In: *Cell Physiology Source Book*, edited by N. Sperelakis. New York: Academic, 1995, p. 180–211.
6. **Blaustein, M. P.** Physiological effects of endogenous ouabain: control of intracellular Ca^{2+} stores and cell responsiveness. *Am. J. Physiol.* 264 (*Cell Physiol.* 33): C1367–C1387, 1993.
7. **Borst-Pauwels, G. W. F. H.** Mutual interaction of ion uptake and membrane potential. *Biochim. Biophys. Acta* 1145: 15–24, 1993.
8. **Byrne, J. H., and S. G. Schultz.** *An Introduction to Membrane Transport and Bioelectricity*. Raven Press, New York, 1988, 66–92.
9. **Chamberlin, M. E., and K. Strange.** Anisosmotic cell volume regulation: a comparative view. *Am. J. Physiol.* 257 (*Cell Physiol.* 26): C159–C173, 1989.
10. **Chapman, I. B., E. A. Johnson, and J. M. Kootsey.** Electrical and biochemical properties of an enzyme model of the sodium pump. *J. Membr. Biol.* 74: 139–153, 1983.
11. **Colclasure, G. C., and J. C. Parker.** Cytosolic protein concentration is the primary volume signal for swelling-induced [K-Cl] cotransport in dog red cells. *J. Gen. Physiol.* 100: 1–10, 1992.
12. **De Smet, P., J. Simaels, and W. Van Driessche.** Regulatory volume decrease in a renal distal tubular cell line (A6). I. Role of K^+ and Cl^-. *Pflügers Arch.* 430: 936–944, 1995.
13. **De Weer, P., and D. Geduldig.** Contribution of sodium pump to resting potential of squid giant axon. *Am. J. Physiol.* 235 (*Cell Physiol.* 4): C55–C62, 1978.
14. **Easterby, J. S.** A generalized theory of the transition time for sequential enzyme reactions. *Biochem. J.* 199: 155–161, 1981.
15. **Easterby, J. S.** The effect of feedback on pathway transient response. *Biochem. J.* 233: 871–875, 1986.
16. **Fisone, G., G. L. Snyder, J. Fryckstedt, M. J. Caplan, A. Aperia, and P. Greengard.** Na^+,K^+-ATPase in choroid plexus. Regulation by serotonin/protein kinase C pathway. *J. Biol. Chem.* 270: 2427–2430, 1995.
17. **Goldman, D. E.** Potential, impedance and rectification in membranes. *J. Gen. Physiol.* 27: 37–60, 1943.
18. **Greger, R.** Cellular membrane transport mechanisms. In: *Comprehensive Human Physiology*, edited by R. Greger and U. Windhorst. Berlin: Springer-Verlag, 1996, p. 149–171.
19. **Grinstein, S., A. Rothstein, B. Sarkadi, and E. W. Gelfand.** Responses of lymphocytes to anisotonic media: volume-regulating behavior. *Am. J. Physiol.* 246 (*Cell Physiol.* 15): C204–C215, 1984.
20. **Hallows, K. R., and P. A. Knauf.** Principles of cell volume regulation. In: *Cellular and Molecular Physiology of Cell Volume Regulation*, edited by K. Strange. Boca Raton, FL: CRC, 1994, p. 3–29.
21. **Häussinger, D.** The role of cellular hydration in the regulation of cell function. *Biochem. J.* 313: 697–710, 1996.
22. **Hernández, J. A., J. Fischbarg, and L. S. Liebovitch.** Kinetic model of the effects of electrogenic enzymes on the membrane potential. *J. Theor. Biol.* 137: 113–125, 1989.
23. **Hill, T. L.** *Free Energy Transduction in Biology*. New York: Academic, 1977, p. 1–32.
24. **Hodgkin, A. L., and B. Katz.** The effect of sodium ions on the electrical activity of the giant axon of the squid. *J. Physiol. (Lond.)* 108: 37–77, 1949.
25. **Hoffman, E. K., I. H. Lambert, and L. O. Simonsen.** Separate, Ca^{2+}-activated K^+ and Cl^- transport pathways in Ehrlich ascites tumor cells. *J. Membr. Biol.* 91: 227–244, 1986.
26. **Hoffman, E. K., and L. O. Simonsen.** Membrane mechanisms in volume and pH regulation in vertebrate cells. *Physiol. Rev.* 69: 315–382, 1989.
27. **Ince, C., B. Thio, B. van Duijn, J. T. van Dissel, D. L. Ypey, and P. C. J. Leijh.** Intracellular K^+, Na^+ and Cl^- concentrations and membrane potential in human monocytes. *Biochim. Biophys. Acta* 905: 195–204, 1987.
28. **Jacquez, J. A.** A generalization of the Goldman equation, including the effects of electrogenic pumps. *Math. Biosci.* 12: 185–196, 1971.
29. **Jakobsson, E.** Interactions of cell volume, membrane potential, and membrane transport parameters. *Am. J. Physiol.* 238 (*Cell Physiol.* 7): C196–C206, 1980.
30. **Kleinzeller, A., and A. Knovotka.** The effect of ouabain on the electrolyte and water transport in kidney cortex and liver slices. *J. Physiol. (Lond.)* 175: 172–192, 1964.
31. **Kregenow, F. M.** Osmoregulatory salt transporting mechanisms: control of cell volume in anisotonic media. *Annu. Rev. Physiol.* 43: 493–505, 1981.

31a. **Kwon, H. M., and J. S. Handler.** Cell volume regulated transporters of compatible osmolytes. *Curr. Opin. Cell Biol.* 7: 465–471, 1995.

32. **Lehninger, A. L., D. L. Nelson, and M. M. Cox.** *Principles of Biochemistry* (2nd ed.). New York: Worth, 1993, p. 375–377.
33. **Lemieux, D. R., F. A. Roberge, and D. Joly.** Modeling the dynamic features of the electrogenic Na,K pump of cardiac cells. *J. Theor. Biol.* 154: 335–358, 1992.
34. **Lemieux, D. R., F. A. Roberge, and P. Savard.** A model study of the contribution of active Na-K transport to membrane repolarization in cardiac cells. *J. Theor. Biol.* 142: 1–34, 1990.
35. **Lew, V. L., and R. M. Bookchin.** Volume, pH and ion-content regulation in human red cells: analysis of transient behavior with an integrated model. *J. Membr. Biol.* 92: 57–74, 1986.
36. **Linshaw, M. A., and F. B. Stapleton.** Effect of ouabain and colloid osmotic pressure on renal tubule cell volume. *Am. J. Physiol.* 235 (*Renal Fluid Electrolyte Physiol.* 4): F480–F491, 1978.
37. **MacKnight, A. D. C.** Volume maintenance in isosmotic conditions. *Curr. Top. Membr. Transp.* 30: 3–43, 1987.
38. **Minton, A. P., G. C. Colclasure, and J. C. Parker.** Model for the role of macromolecular crowding in regulation of cellular volume. *Proc. Natl. Acad. Sci. USA* 89: 10504–10506, 1992.
39. **Mizraji, E., L. Acerenza, and J. A. Hernández.** Time delays in metabolic control systems. *Biosystems* 22: 11–17, 1988.
41. **Moreton, R. B.** An investigation of electrogenic sodium pump in snail neurons using the constant field theory. *J. Exp. Biol.* 51: 181–201, 1969.
42. **Mullins, N. J., and K. Noda.** The influence of sodium-free solutions on the membrane potential of frog muscle fibers. *J. Gen. Physiol.* 47: 117–132, 1963.
43. **Olivotto, M., A. Arcangeli, M. Carlà, and E. Wanke.** Electric fields at the plasma membrane level: a neglected element in the mechanisms of cell signalling. *Bioessays* 18: 495–504, 1996.
44. **Palfrey, H. C.** Protein phosphorylation control in the activity of volume-sensitive transport systems. In: *Cellular and Molecular Physiology of Cell Volume Regulation*, edited by K. Strange. Boca Raton, FL: CRC, 1994, p. 201–214.
45. **Parker, J. C.** In defense of cell volume? *Am. J. Physiol.* 265 *(Cell Physiol.* 34): C1191–C1200, 1993.
46. **Parker, J. C.** Coordinated regulation of volume-activated transport pathways. In: *Cellular and Molecular Physiology of Cell Volume Regulation*, edited by K. Strange. Boca Raton, FL: CRC, 1994, p. 311–321.
47. **Rodríguez-Boulan, E., and W. J. Nelson.** Morphogenesis of the polarized epithelial cell phenotype. *Science* 245: 718–725, 1989.
48. **Rossier, B. C., K. Geering, and J. P. Kraehenbuhl.** Regulation of the sodium pump: how and why? *Trends Biochem. Sci.* 12: 483–487, 1987.
49. **Schultz, S. G.** *Basic Principles of Membrane Transport*. Cambridge, UK: Cambridge University Press, 1980.
50. **Scriven, D. R.** Modeling repetitive firing and bursting in a small unmyelinated nerve fiber. *Biophys. J.* 35: 715–730, 1981.
51. **Segel, G. B., W. Simon, and M. A. Lichtman.** Regulation of sodium and potassium transport in phytohemagglutinin-stimulated human blood lymphocytes. *J. Clin. Invest.* 64: 834–841, 1979.
52. **Severini, A., K. V. S. Prasad, A. F. Almeida, and J. G. Kaplan.** Regulation of the number of K^+,Na^+-pump sites after mitogenic activation of lymphocytes. *Biochem. Cell Biol.* 65: 95–104, 1987.
53. **Sjodin, R. A.** Contribution of electrogenic pumps to resting membrane potentials: the theory of electrogenic potentials. In: *Electrogenic Transport: Fundamental Principles and Physiological Implications*, edited by M. P. Blaustein and M. Lieberman. New York: Raven, 1984, p. 105–127.

54. **Sperelakis, N.** Diffusion and permeability. In: *Cell Physiology Source Book*, edited by N. Sperelakis. New York: Academic, 1995, p. 61–66.
55. **Strieter, J., J. L. Stephenson, L. G. Palmer, and A. M. Weinstein.** Volume-activated chloride permeability can mediate cell volume regulation in a mathematical model of a tight epithelium. *J. Gen. Physiol*. 96: 319–344, 1990.
56. **Tosteson, D. C., and J. F. Hoffman.** Regulation of cell volume by active cation transport in high and low potassium sheep red cells. *J. Gen. Physiol*. 44: 169–194, 1960.
57. **Verkman, A. S.** Water channels in cell membranes. *Annu. Rev. Physiol*. 54: 97–108, 1992.
58. **Weinstein, A. M.** Analysis of volume regulation in an epithelial cell model. *Bull. Math. Biol*. 54: 537–561, 1992.
59. **Weinstein, A. M.** A kinetically defined Na^+/H^+ antiporter within a mathematical model of the rat proximal tubule. *J. Gen. Physiol*. 105: 617–641, 1995.
60. **Weinstein, A. M.** Dynamics of cellular homeostasis: recovery time for a perturbation from equilibrium. *Bull. Math. Biol*. 59: 451–481, 1997.
61. **Welling, D. J., and L. W. Welling.** Model of renal cell volume regulation without active transport: role of a heteroporous membrane. *Am. J. Physiol*. 255 (*Renal Fluid Electrolyte Physiol*. 24): F529–F538, 1988.
62. **Yancey, P. H., M. E. Clark, S. C. Hand, R. D. Bowlus, and G. N. Somero.** Living with water stress: evolution of osmolyte systems. *Science* 217: 1214–1222, 1982.